

---

# ClimDetect: A Benchmark Dataset for Climate Change Detection and Attribution

---

Sungduk Yu<sup>1</sup>\*, Brian L. White<sup>2</sup>, Anahita Bhiwandiwalla<sup>1</sup>, Musashi Hinck<sup>1</sup>,  
Matthew Lyle Olson<sup>1</sup>, Tung Nguyen<sup>3</sup>, Vasudev Lal<sup>1</sup>

<sup>1</sup>Intel Labs, <sup>2</sup>UNC Chapel Hill, <sup>3</sup>UCLA

## Abstract

Detecting and attributing temperature increases due to climate change is crucial for understanding global warming and guiding adaptation strategies. The complexity of distinguishing human-induced climate signals from natural variability has challenged traditional detection and attribution (D&A) approaches, which seek to identify specific "fingerprints" in climate response variables. Deep learning offers potential for discerning these complex patterns in expansive spatial datasets. However, lack of standard protocols has hindered consistent comparisons across studies. We introduce *ClimDetect*, a standardized dataset of over 816k daily climate snapshots, designed to enhance model accuracy in identifying climate change signals. *ClimDetect* integrates various input and target variables used in past research, ensuring comparability and consistency. We also explore the application of vision transformers (ViT) to climate data, a novel and modernizing approach in this context. Our open-access data and code serve as a benchmark for advancing climate science through improved model evaluations. *ClimDetect* is publicly accessible via Huggingface dataet repository at: <https://huggingface.co/datasets/ClimDetect/ClimDetect><sup>2</sup>.

## 1 Introduction

Climate change, particularly the increase in global temperature in response to anthropogenic greenhouse gas emissions, has emerged as one of the most pressing environmental challenges of the 21st century. The Intergovernmental Panel on Climate Change (IPCC) has highlighted the importance of understanding the drivers of these changes in order to implement effective mitigation and adaptation strategies [1]. A key challenge in climate science has been developing methodologies for the detection and attribution (D&A) of climate signals, in order to differentiate human-induced warming from natural climate variability [2–4].

Traditional approaches in climate D&A have leveraged statistical methods to discern climate "fingerprints", or patterns in climate response variables that can be attributed to external forcing, such as greenhouse gas emissions. Many studies have used principal component analysis (PCA; also known as empirical orthogonal functional, EOF, analysis in the climate community) to derive spatial fingerprints from long-term climate ensembles [5–7]. However, recent studies have advanced the state of the art, for example by showing it is possible to detect the climate change signal in daily snapshots of global weather [8, 9], and by leveraging the advantages of machine learning for pattern recognition [e.g., 10–13] to learn spatial fingerprints and forced climate response directly from large climate datasets. These recent result show that deep learning can provide useful tools for D&A, due to

---

\*[sungduk.yu@intel.com](mailto:sungduk.yu@intel.com)

<sup>2</sup>available under CC BY 4.0 License

the ability of models to uncover intricate patterns in large climate datasets. However, the application of sophisticated models requires large, diverse and balanced dataset that encapsulates a wide range of climate response variables, forcing metrics, natural variability, and climate models.

In response to these needs, we introduce ‘ClimDetect’, a comprehensive dataset designed to facilitate and standardize climate change fingerprinting (Figure 1). This dataset combines over 816,000 daily snapshots of historical and future climate scenarios from the Coupled Model Intercomparison Project Phase 6 (CMIP6) model ensemble, carefully curated by subject matter experts to foster the development of models capable of detecting climate change signals in daily weather patterns. ClimDetect aims to address the fragmentation in previous studies by standardizing the input and target variables used in climate fingerprinting, promoting consistency and comparability across D&A research efforts. Our research extends current understanding beyond traditional methodologies by incorporating modern machine learning architectures, i.e. Vision Transformers (ViT) [14], into climate science. ViTs have shown amazing performance on natural image tasks and are adapted in our study to analyze spatial climate data.

By providing open access to the ClimDetect dataset and the associated analytical code, our work sets a benchmark for future studies, encouraging the exploration of diverse modeling techniques in the climate science community. With this work, we hope to foster scientific research and addresses societal goals by deepening understanding and mitigation of climate change impacts. By using ClimDetect, scientists can obtain clearer insights into climate dynamics, supporting global efforts to address this critical challenge.

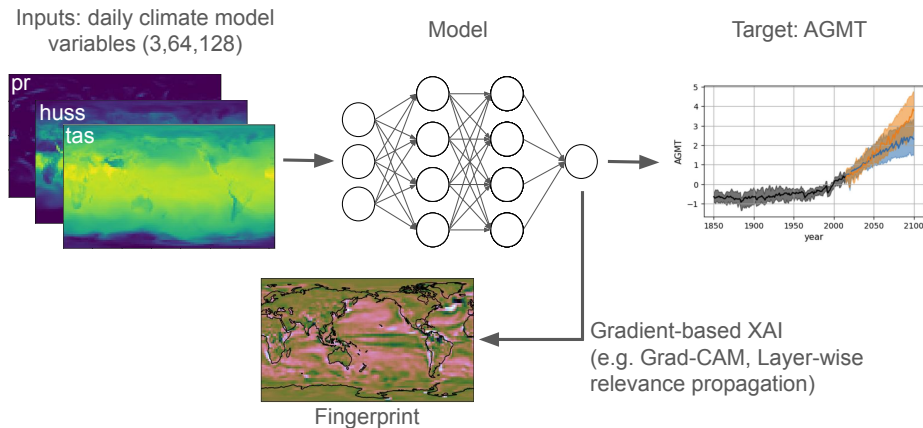


Figure 1: Overview of the machine learning pipeline for climate change detection and attribution using the ClimDetect dataset. The diagram illustrates the workflow from input daily climate model variables (surface air temperature, humidity, precipitation), through a neural network model, to the target annual global mean temperature (AGMT). Key components include the model’s architecture, output AGMT projections, and application of gradient-based explainable AI (XAI) techniques, such as Grad-CAM and layer-wise relevance propagation, to generate a ‘fingerprint’ that identifies influential features in climate data related to human-caused changes.

## 2 Background and Related Work

### 2.1 Concepts and Terminology from Climate Science

To motivate the problem of climate D&A, it is important to first clarify fundamental concepts and terminologies, including: natural climate variability, CMIP6 climate projections [18]. Figure 2 shows these concepts applied to representative data from the ClimDetect dataset. Predictions of a target variable representing climate forcing (in this case, annual global mean temperature, AGMT) are shown from a model (ViT-b/16) trained on daily climate variables from the ClimDetect dataset. Input data span historical and future climate scenarios, illustrating warming trends, while confidence intervals illustrate the range of climate variability. The sensitivity of an ML model for D&A can be measured by its ability to reduce the error in the AGMT prediction relative to the variability of background climate.

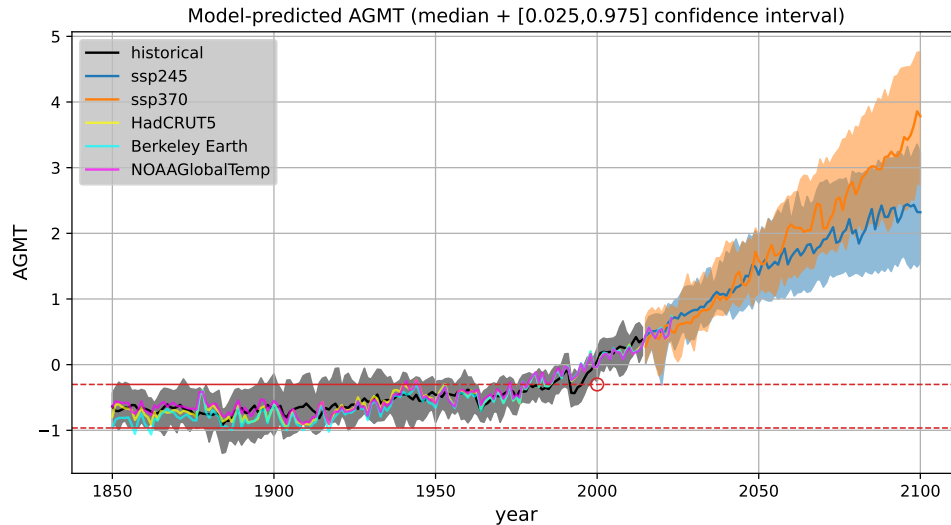


Figure 2: Annual global mean temperature over time from observations (HadCRUT5[15], Berkeley Earth[16], NOAAGlobalTemp[17]) and from model (ViT-b/16) predictions made from daily weather variables from CMIP6 models in the ClimDetect test set over historical and projected (SSP245, SSP370) climate. The values are relative to the 1980-2014 average. Shaded regions represent the [2.5%, 97.5%] confidence intervals from the model prediction. The mean of the CI over the historical period 1850-1950 (solid red line and extended dashed red line) represents the range of the baseline pre-industrial climate and the CI range represents background climate variability. The red circle illustrates the time period during which the warming signal emerges from the range of background climate variability – even from a daily weather snapshot [e.g., 8, 9, 13]. Models which can reduce the variance in the AGMT target prediction relative to the internal climate variability will be more sensitive to this emergence and hence be more accurate in D&A.]

**Natural Climate Variability (Internal Variability).** Natural climate variability, or internal variability, refers to the inherent fluctuations in the climate state caused by the internal dynamics of the Earth’s climate system. These fluctuations occur across various timescales, from seasonal to multi-decadal, and are independent of external forcing factors like volcanic eruptions or human-induced greenhouse gas emissions. Such variability is driven by complex interactions within the climate system, including the atmosphere, oceans, cryosphere, and land surfaces. For example, the El Niño-Southern Oscillation (ENSO), Pacific Decadal Oscillation and the Atlantic Multi-decadal Oscillation each affect global weather over multi-year timescales. Understanding these patterns is crucial for distinguishing between changes in climate due to external forcings and those arising from the climate system’s inherent dynamics.

**CMIP6 Climate Projections.** CMIP6 is a globally coordinated effort with over 100 climate models from more than 50 groups, making it a comprehensive climate modeling project [18]. With data exceeding 20 petabytes, CMIP6 is integral to the IPCC Assessment Reports [1], which inform climate change assessments for policymakers and scientists. It includes key ‘historical’ and ‘scenarioMIP’ experiments; historical simulations replicate the climate from 1850 to 2014 using data like greenhouse gas concentrations and land use changes, elucidating the impact of natural and human activities on climate over the past 150 years. ScenarioMIP projects future climates from 2015 to 2100 under various Shared Socioeconomic Pathways (SSPs), such as SSP2-4.5 (moderate) and SSP3-7.0 (high-emission), helping explore the outcomes of different climate actions. Our study processes and leverages this detailed dataset to support our research objectives.

## 2.2 Related work

**Climate Detection and Attribution Studies.** Previous work D&A within the climate science community has focused on distinguishing between the climate signal and internal variability by finding spatial fingerprints. But methodologies have varied by: 1) the statistical / modeling approach

used to discover the fingerprint, 2) The climate time-scales of focus, 3) the climate response variables under study, and 4) the target metric chosen to represent the climate forcing.

Santer et al. [5] use PCA (EOF) analysis to investigate the climate fingerprint of climate variables, including water vapor [6] and tropospheric temperature [7]. They project observations onto the leading PCA modes from climate model ensembles to show statistical significance vs. control runs without greenhouse gas forcing, primarily examining multi-decadal periods.

Sippel et al. find climate fingerprints from daily weather variables (surface temperature and humidity), by regularized linear (ridge) regression [8] and anchor regression [9] on large ensembles of CMIP5/6 models, using AGMT as the target metric. They project the daily variables (temperature alone or mean-removed temperature and humidity) onto the fingerprints to predict current observations, which are then compared against predictions of the target metric in a pre-warming (1850-1950) climate.

Barnes and co-authors [10, 11] use machine learning to find the spatial pattern of warming, framed as classification task. They train on a large climate model ensemble (CMIP5) with annual temperature and precipitation as inputs, using an MLP to predict the model year [10, 11]. They define detectability as the "time of emergence", relative to a baseline control period (1920–1959) [12] and use interpretable ML (layer-wise relevance propagation [e.g., 11, 12, 19] and backward optimization [11, 20]) to visualize the learned spatial patterns. Ham et al. [13] use a CNN to predict AGMT using precipitation only, a much weaker signal compared with temperature. The performance of the CNN shows the potential for deep learning to develop more sensitive D&A methods.

The previous works illustrate the potential benefit of standardized data sets and test methods for improving and comparing D&A methods. We develop `ClimDetect` specifically to address these needs, focusing on a developing a balanced and diverse dataset.

**Climate Datasets for ML.** A number of previous works have created large climate and weather datasets for the purpose of training and bench-marking deep learning models. Datasets like WeatherBench[21], WeatherBench2 [22], and ChaosBench [23] have advanced ML weather prediction by creating consistent benchmark datasets for weather forecasting with different forecast horizons, helping to facilitate a paradigm shift whereby data-driven forecasts [e.g., 24–27] are reaching parity with traditional numerical weather forecast models.

Benchmark datasets for climate modeling include ClimSim [28], the largest ever dataset for hybrid physics-ML modeling. ClimSim enables the development of ML emulators to address the critical problem of improving convective parameterization for cloud and rainfall processes in climate models. ClimateBench [29] is an ML-ready benchmark dataset for climate emulation, consisting of climate forcing variables (CO<sub>2</sub>, CH<sub>4</sub>, SO<sub>2</sub>) and outputs from a single model in the CMIP6 archive over a suite of forcing scenarios. It enables the training of models to predict future annual-mean climate data (e.g. temperature and precipitation) from the forcing data. Kaltenborn et al. [30] created ClimateSet, a new ML-ready dataset for climate emulation, expanding to 36 climate models from CMIP6 archive, with monthly data for forcing and output climate variables, over historical and future scenarios. Nguyen et al. [31] developed ClimateLearn, an open-source PyTorch library to train and evaluate ML climate and weather models.

### 3 ClimDetect

We develop `ClimDetect`, a dataset of 816k daily snapshots from the CMIP6 model ensemble to enable D&A studies over different climate response variables and target variables that represent climate forcing. The dataset spans 28 different climate models and 142 specific model ensemble runs spanning historical (1850-2014) and SSP2-4.5 and SSP3-7.0. scenarios. The data is chosen to emphasize diversity and balance, covering a range of models with different physics, and a range of climate forcing scenarios. The climate variables chosen to represent the *daily* snapshots, surface 2-meter temperature (tas), surface 2-meter specific humidity (huss) and total precipitation (pr), are climate response variables of broad interest and which have been the focus of previous D&A studies [8–11, 13].

We use the `ClimDetect` dataset to frame the D&A problem as an ML regression task. Following recent work by [8, 9, 13], we use *daily* climate fields from CMIP6 model output to predict a scalar value, AGMT, as a proxy for the climate forcing signal.

The inputs to the model are a 3-dimensional matrix  $\mathbf{X}$  with dimensions  $64 \times 128 \times 3$ . The matrix  $\mathbf{X}$  represents a 64x128 grid over latitude and longitude, with the three channels corresponding to tas, huss and pr. Mathematically, the input matrix  $\mathbf{X}$  can be expressed as:  $\mathbf{X} \in \mathbb{R}^{64 \times 128 \times 3}$ . The model processes this input to predict the scalar outcome  $\text{AGMT} = f(\mathbf{X})$  where  $f$  denotes the function learned by the model.

The evaluation metric for the regression task (and for the benchmark—see Section 4) is RMSE, evaluated on the test set (consisting of a blend of historical and SSP245, 370 model projections). Sippel et al. [8] show that the RMSE from daily predictions of AGMT is a good proxy for signal-to-noise improvement relative to background climate variability (see also Figure 2).

### 3.1 Data Collection

To construct the `ClimDetect` dataset, we utilized data from the CMIP6 [18], specifically leveraging the historical and ScenarioMIP experiments. Within the ScenarioMIP, we selected two prevalent scenarios, SSP245 ("Middle of the Road") and SSP370 ("Regional Rivalry"), which are representative of moderate and high greenhouse gas emissions trajectories, respectively.

Given that participation in CMIP6 is voluntary, the availability of simulated climate variables and the number of ensemble simulations differ across the various climate models. To ensure consistency and reliability in our dataset, we implemented a three of criteria for model selection.

**Model Requirements:** Each model must include simulations from the historical experiment covering the entire simulation period from 1850 to 2014, as well as from at least one of the selected ScenarioMIP experiments (SSP245 and SSP370) for the period from 2015 to 2100.

**Variable Availability:** It is essential that all three key climate variables—surface air temperature, surface air humidity, and total precipitation rate—are available for each simulation. This criterion guarantees that our dataset consistently represents the primary factors influencing global climate patterns.

**Temporal Coverage:** The models selected must provide data for the entire duration of the specified experiments, ensuring comprehensive coverage and facilitating accurate long-term climate analysis.

By adhering to these stringent selection criteria, we aim to maximize the robustness and applicability of the `ClimDetect` dataset, enabling detailed analysis and modeling of climate dynamics under various emission scenarios as projected by CMIP6. All CMIP6 data was accessed from the Registry of Open Data on AWS (<https://registry.opendata.aws/cmip6/>) available under CC BY 4.0 License.

### 3.2 Postprocessing

`ClimDetect` aims to provide a machine learning (ML)-ready dataset, and as such, has undergone specific preprocessing steps to ensure the data is standardized for optimal ML model performance. The preprocessing of input variables adheres to a method akin to z-score standardization, tailored to address the unique characteristics of climate data. The preprocessing involves two primary steps:

**Removal of the Climatological Daily Seasonal Cycle.** Each input variable  $x$ , which is represented as a three-dimensional array with dimensions [channel, latitude, longitude], is adjusted to remove the climatological daily seasonal cycle, denoted as  $x_{\text{clim}}$ . This step encourages analysis on anomalies rather than absolute values, which can be heavily influenced by seasonal effects. Mathematically, the anomaly  $x'$  for each data point is calculated as:  $x' = x - x_{\text{clim}}$  where  $x_{\text{clim}}$  represents the long-term average for that particular day at each channel, latitude, and longitude point, effectively normalizing the data across years to highlight deviations from typical patterns.

**Standardization of Anomalies.** The computed anomalies  $x'$ , still maintaining the [channel, latitude, longitude] structure, are then standardized by dividing each by its temporal standard deviation  $\sigma_{x'}$  computed over the same dimensions. This scaling transforms the data into a form where the variance is normalized across the dataset:  $z = x' / \sigma_{x'}$ . Here,  $z$  represents the standardized value, which aligns with the principles of z-score standardization.

The  $x_{\text{clim}}$  and  $\sigma_{x'}$  values are calculated based on the period from 1980 to 2014 using historical simulations and are specific to each model because each model has different background climate largely due to different model physics and numerical schemes. These preprocessing steps ensure

that the dataset is not only cleansed of inherent seasonal biases but also standardized in a manner conducive to extracting meaningful patterns through ML techniques.

### 3.3 Dataset Split and Access

The `ClimDetect` dataset, encompassing a total of 816,213 samples, is carefully divided into training, validation, and testing subsets to facilitate effective model training, parameter tuning, and performance evaluation. Specifically, 77% of the samples (627,581 samples) are allocated to the training dataset, 10% (80,227 samples) to the validation dataset, and the remaining 13% (108,405 samples) to the testing dataset. We also provide a "mini" version of the dataset for the purpose of prototyping with 12,468 / 2,985 / 2,985 observations in train / validation / test splits.

When distributing the climate models across these subsets, a key consideration is the "climate sensitivity" of each model [32, 33]. Climate sensitivity refers to a model's responsiveness to climate forcings, such as greenhouse gases, which can cause variations in the projected warming. Models vary in their climate sensitivity; some predict higher temperatures under the same forcing scenarios (more sensitive), while others forecast less warming (less sensitive). To ensure a comprehensive and balanced evaluation, we have deliberately selected models across the entire spectrum of climate sensitivity for each dataset split.

The `ClimDetect` dataset is structured using the Hugging Face Datasets library, ensuring it is fully integrated with the Hugging Face ecosystem.

## 4 Benchmark

The benchmark experiments designed for the `ClimDetect` dataset (Table 1) aim to comprehensively evaluate the effectiveness of using different combinations of climate variables to predict AGMT. The primary experiment, named "tas-huss-pr," utilizes all three `ClimDetect` variables—surface temperature, surface humidity, and total precipitation rate—as inputs to estimate AGMT. This experiment serves as the foundation for understanding the combined predictive power of these variables.

In addition to the "tas-huss-pr" experiment, we conducted a series of supplementary experiments to explore the predictive utility of individual variables, reflecting common approaches in prior studies. These experiments are categorized under the single-variable setup, where each experiment uses only one of the three available variables. Specifically, we have the "tas\_only" experiment using only surface temperature, the "huss\_only" experiment focusing solely on surface humidity, and the "pr\_only" experiment that considers only the total precipitation rate. Each of these experiments provides insights into the individual contributions of the variables to the accuracy of AGMT predictions.

Furthermore, we included two "mean-removed" ("mr") experiments, which are modifications of the "tas-huss-pr" and "tas\_only" setups. In these experiments, the spatial mean of each climate field snapshot is removed before conducting the analysis. The rationale behind these "mean-removed" experiments stems from the work of Santer et al. [7] and Sippel et al. [8], which suggest that removing the global mean changes can reveal more about the spatial patterns that contribute to climate signal detection. This approach is predicated on the idea that focusing on spatial anomalies, rather than spatially-averaged residual values, can enhance the detection of climate change signals based on the similarity of spatial patterns alone, thereby increasing confidence in the detection outcomes.

### 4.1 Baseline Models and Training Details

Using the `ClimDetect` dataset, we apply a collection of ViT-based models to the fingerprinting problem. To do this, we add a regression head to a pretrained ViT checkpoint, jointly finetune the regression head and model on the train split of the `ClimDetect` dataset, and then apply GradCAM to the penultimate layer of the transformer stack.

We use the following pre-trained ViT-based checkpoints: `google/vit-base-patch16-224` ViT-b/16 model [14]; `openai/clip-vit-large-patch14-336` image encoder [34]; `facebook/vit-mae-base` image encoder [35]; and `facebook/dinov2-large` DinoV2 model [36]. The remaining two models are a basic multi-layer perceptron (MLP) and a ridge regression.

Experiment Name	Input Variables	Target Variable	Mean Removed
tas-huss-pr	tas, huss, pr	AGMT	No
tas_only	tas	AGMT	No
huss_only	huss	AGMT	No
pr_only	pr	AGMT	No
tass-huss-pr_mr	tas, huss, pr	AGMT	Yes
tas_mr	tas	AGMT	Yes

Table 1: Summary of Benchmark Experiments for ClimDetect Dataset. tas: surface air temperature, huss: surface air specific humidity, pr: total precipitation rate, AGMT: annual global mean temperature.

These ViT models and checkpoints are widely used in the computer vision and multimodal literatures [37] and cover a diverse set of pretraining approaches to a common architecture. Adjustments specific to our climate data involved fine-tuning with a uniform batch size of 64 and a learning rate of  $5e-4$ , optimized through a grid search initially conducted on Google’s ViT-b/16 [14]. We trained for 10 epochs using the AdamW optimizer updating all parameters of the model. Total training took 4.75 hours on average per model using eight A6000 Nvidia GPUs on an internal linux slurm cluster. We additionally investigated training our own ViT model from scratch over the training data, but found that despite four times increased training cost, validation error was worse than starting with an existing foundation model. We provide additional details on the training in the supplementary materials.

To provide a comprehensive evaluation, traditional models used in climate science were also included: a ridge regression model and a multilayer perceptron (MLP). The ridge regression was tuned with a large alpha value ( $10^6$ ), while the MLP featured five hidden layers with 100 units each, a learning rate of  $5e-5$  with cyclic learning rate adjustments, and L2 regularization with  $\alpha=0.01$ . These models served as benchmarks to assess the state-of-the-art capabilities of ViT models against conventional methods in the context of climate change detection and attribution.

## 4.2 Results

The RMSE analysis conducted across six experiments with six models, including four ViTs, one MLP, and one ridge regression, illustrates a competitive landscape with relatively close performances among the models. Notably, ViTs consistently outperform simpler models such as MLP and Ridge Regression in experiments involving multiple variables, such as tas-huss-pr and tas-huss-pr\_mr. These results suggest that ViTs may be better suited for modeling the complex and high-order interactions underlying the data generating process for multiple climate variables.

Experiments that involved removing the mean signal (mean-removed experiments) posed greater challenges for all models, reflecting the increased difficulty of making predictions without the data provided by mean residual signals. Despite this, ViTs maintained a relatively strong performance, indicating their capability to utilize spatial anomalies effectively. However, in the pr\_only experiment, where models were tasked with using only precipitation data, all models, particularly Ridge Regression, struggled likely due to the sparsity and indirect relationship of precipitation with climate state variables (e.g., temperature and humidity).

These findings underscore the potential of ViTs in future climate detection and attribution studies, especially in scenarios that leverage multiple variables and complex data configurations – although the overall choice of model should still consider specific experiment requirements and data characteristics.

## 4.3 Physical Interpretation

In order to conduct a fingerprinting analysis with ViTs, we utilize a popular attribution metric from the computer vision literature: Gradient-weighted Class Activation Mapping (Grad-CAM) [38]. Grad-CAM provides visual explanations for model decisions by highlighting the areas within input data that significantly influence predictions. To facilitate this, we categorized the test dataset samples into four bins based on their AGMT values, with bin edges set at  $[-0.5, 0.5, 1.5, 2.5, 3.5]$ , encompassing about 90% of the data distribution. This binning approach allowed us to systematically examine how

Model	tas-huss-pr	tas_only	pr_only	huss_only	tas-huss-pr_mr	tas_mr
ViT-b/16	0.1425	0.1610	0.7132	0.1604	0.1763	0.2562
CLIP	<b>0.1411</b>	<b>0.1482</b>	0.8935	0.1801	0.1690	0.2410
MAE	0.1430	0.1484	<b>0.6451</b>	<b>0.1571</b>	<b>0.1672</b>	0.2531
DINOv2	0.1439	0.1645	0.7995	0.1942	0.1731	0.2552
MLP	0.1488	0.1557	0.7502	0.1804	0.2192	0.2409
Ridge	0.1508	0.1542	0.9708	0.2304	0.2156	<b>0.2404</b>

Table 2: RMSE Values Across Different Models and Experiments (Unit: °C). A matching table for  $R^2$  is in the supplementary materials.

the model’s focus shifts across different temperature scenarios, providing insights into the relevance of specific climatic features as interpreted by our models. Figure 3 shows the results of the physical interpretation on a variety our tas\_only models for the [1.5,2.5] bin, showing a large difference in important features between models. We present comprehensive Grad-CAM results (all experiments and all bins) in the supplementary materials.

Additionally, we included visualizations of ridge regression coefficients to serve as a first-order baseline comparison for interpretability. These coefficients illustrate the linear relationships within the input data, with smoothed maps highlighting significant climatic hotspots such as the North Atlantic warming hole and specific oceanic and continental regions. In contrast, the Grad-CAM visualizations for models like CLIP, MAE, ViT-b/16, and DINOv2 present diverse insights, reflecting different internal processing patterns despite similar RMSE scores. Notably, the DINOv2 model shows a Grad-CAM pattern that closely resembles the spatial pattern captured by the ridge regression, particularly capturing relevant features such as the North Atlantic warming hole and showing minimal relevance over the polar regions.

These findings highlight the nuanced capabilities of ViTs in climate detection and attribution, with the DINOv2 model demonstrating particularly promising results that align closely with traditional linear interpretations. However, the varied results across different ViT models suggest a need for further investigation into their architectural specifics and potential adjustments to enhance their interpretive accuracy. Future work should extend beyond Grad-CAM to include other interpretative tools and investigate deeper into the specifics of ViT architectures to fully harness their potential in climate science.

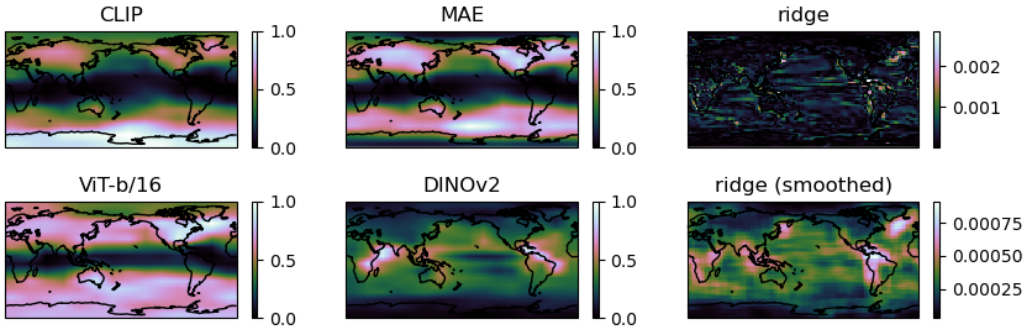


Figure 3: (left and middle panels) Grad-CAM visualizations for CLIP, MAE, ViT-b/16, DINOv2 models for the tas\_only experiment, highlighting regions of significant influence on the prediction of output (Annual Global Mean Temperature, AGMT). GradCAM was calculated for each test set samples whose AGMT falls within [1.5,2.5], and then averaged. (right panels) Ridge regression coefficients and their smoothed version using a 8x8 window, showing linear relationships between local pixel and the AGMT.

## 5 Limitations and Future Work

ClimDetect is designed to offer a standardized dataset for generating climate change fingerprints, effectively utilizing a broad range of variables to enhance model training and analysis. To further

extend its applicability and robustness, we plan to introduce “ClimDetect-Obs”, an expansion that will incorporate observational and reanalysis (which is observation-blended model output) datasets. And while not the main focus of this study, we acknowledge the limitations in directly comparing GradCAM visualizations for Vision Transformers (ViTs) with linear model coefficients. The intrinsic complexity of ViTs means GradCAM may not adequately reflect their interpretative layers as linear models do. To firmly establish ViTs as tools for climate fingerprinting, further exploration of diverse model interpretation tools is necessary.

## 6 Conclusion

We introduced the ClimDetect dataset, a standardized tool designed to unify and enhance prior efforts in climate change detection and attribution, utilizing consistent input and output variables, datasets, and models from historical and ScenarioMIP experiments of CMIP6. This harmonization enhances comparability and reproducibility across studies while focusing on key variables such as surface temperature, humidity, and precipitation critical for robust climate modeling. Moreover, we have expanded the methodological toolkit of climate science by incorporating a range of models, including ViTs, alongside traditional machine learning techniques. This diverse array of models tests established methods and explores the potential of ViTs to optimize machine learning architectures for climate-related tasks. The ClimDetect dataset not only advances the integration of machine learning in climate science but also sets the stage for future research and policy-making, aiming to tackle global climate change challenges effectively.

## Acknowledgments and Disclosure of Funding

The authors report there are no acknowledgments or funding sources to declare for this study.

## References

- [1] IPCC. *Climate Change 2021: The Physical Science Basis. Contribution of Working Group I to the Sixth Assessment Report of the Intergovernmental Panel on Climate Change*, volume In Press. Cambridge University Press, Cambridge, United Kingdom and New York, NY, USA, 2021. doi: 10.1017/9781009157896.
- [2] E K Schneider and J L Kinter. An examination of internally generated variability in long climate simulations. *Climate Dynamics*, 10(4-5):181–204, 1994. ISSN 0930-7575. doi: 10.1007/bf00208987.
- [3] Clara Deser, Reto Knutti, Susan Solomon, and Adam S. Phillips. Communication of the role of natural variability in future North American climate. *Nature Climate Change*, 2(11):775–779, 2012. ISSN 1758-678X. doi: 10.1038/nclimate1562.
- [4] E. Hawkins and R. Sutton. Time of emergence of climate signals. *Geophysical Research Letters*, 39(1), 2012. ISSN 0094-8276. doi: 10.1029/2011gl050087.
- [5] Benjamin D Santer, Wolfgang Brüggemann, Ulrich Cubasch, Klaus Hasselmann, Heinke Höck, Ernst Maier-Reimer, and Uwe Mikolajewica. Signal-to-noise analysis of time-dependent greenhouse warming experiments. *Climate Dynamics*, 9(6):267–285, 1994. ISSN 0930-7575. doi: 10.1007/bf00204743.
- [6] B. D. Santer, C. Mears, F. J. Wentz, K. E. Taylor, P. J. Gleckler, T. M. L. Wigley, T. P. Barnett, J. S. Boyle, W. Brüggemann, N. P. Gillett, S. A. Klein, G. A. Meehl, T. Nozawa, D. W. Pierce, P. A. Stott, W. M. Washington, and M. F. Wehner. Identification of human-induced changes in atmospheric moisture content. *Proceedings of the National Academy of Sciences*, 104(39): 15248–15253, 2007. ISSN 0027-8424. doi: 10.1073/pnas.0702872104.
- [7] Benjamin D. Santer, Stephen Po-Chedley, Mark D. Zelinka, Ivana Cvijanovic, Céline Bonfils, Paul J. Durack, Qiang Fu, Jeffrey Kiehl, Carl Mears, Jeffrey Painter, Giuliana Pallotta, Susan Solomon, Frank J. Wentz, and Cheng-Zhi Zou. Human influence on the seasonal cycle of tropospheric temperature. *Science*, 361(6399), 2018. ISSN 0036-8075. doi: 10.1126/science.aas8806.

- [8] Sebastian Sippel, Nicolai Meinshausen, Erich M. Fischer, Enikő Székely, and Reto Knutti. Climate change now detectable from any single day of weather at global scale. *Nature Climate Change*, 10(1):35–41, 2020. ISSN 1758-678X. doi: 10.1038/s41558-019-0666-7.
- [9] Sebastian Sippel, Nicolai Meinshausen, Enikő Székely, Erich Fischer, Angeline G. Pendergrass, Flavio Lehner, and Reto Knutti. Robust detection of forced warming in the presence of potentially large climate variability. *Science Advances*, 7(43):eabh4429, 2021. doi: 10.1126/sciadv.abh4429.
- [10] Elizabeth A. Barnes, James W. Hurrell, Imme Ebert-Uphoff, Chuck Anderson, and David Anderson. Viewing Forced Climate Patterns Through an AI Lens. *Geophysical Research Letters*, 46(22):13389–13398, 2019. ISSN 0094-8276. doi: 10.1029/2019gl084944.
- [11] Elizabeth A. Barnes, Benjamin Toms, James W. Hurrell, Imme Ebert-Uphoff, Chuck Anderson, and David Anderson. Indicator Patterns of Forced Change Learned by an Artificial Neural Network. *Journal of Advances in Modeling Earth Systems*, 12(9), 2020. ISSN 1942-2466. doi: 10.1029/2020ms002195.
- [12] Jamin K. Rader, Elizabeth A. Barnes, Imme Ebert-Uphoff, and Chuck Anderson. Detection of Forced Change Within Combined Climate Fields Using Explainable Neural Networks. *Journal of Advances in Modeling Earth Systems*, 14(7), 2022. ISSN 1942-2466. doi: 10.1029/2021ms002941.
- [13] Yoo-Geun Ham, Jeong-Hwan Kim, Seung-Ki Min, Daehyun Kim, Tim Li, Axel Timmermann, and Malte F. Stuecker. Anthropogenic fingerprints in daily precipitation revealed by deep learning. *Nature*, 622(7982):301–307, 2023. ISSN 0028-0836. doi: 10.1038/s41586-023-06474-x.
- [14] Alexey Dosovitskiy, Lucas Beyer, Alexander Kolesnikov, Dirk Weissenborn, Xiaohua Zhai, Thomas Unterthiner, Mostafa Dehghani, Matthias Minderer, Georg Heigold, Sylvain Gelly, et al. An image is worth 16x16 words: Transformers for image recognition at scale. *arXiv preprint arXiv:2010.11929*, 2020.
- [15] Colin P Morice, John J Kennedy, Nick A Rayner, JP Winn, Emma Hogan, RE Killick, RJH Dunn, TJ Osborn, PD Jones, and IR Simpson. An updated assessment of near-surface temperature change from 1850: The hadcrut5 data set. *Journal of Geophysical Research: Atmospheres*, 126(3):e2019JD032361, 2021.
- [16] Robert A Rohde and Zeke Hausfather. The berkeley earth land/ocean temperature record. *Earth System Science Data*, 12(4):3469–3479, 2020.
- [17] B. Huang, X. Yin Yin, M. J. Menne, R. Vose, and H. Zhang. Noaa global surface temperature dataset (noaaglobaltemp), version 6.0.0. noaa national centers for environmental information, 2023. URL <https://www.ncei.noaa.gov/metadata/geoportal/rest/metadata/item/gov.noaa.ncdc%3AC01704/html>.
- [18] Veronika Eyring, Sandrine Bony, Gerald A. Meehl, Catherine A. Senior, Bjorn Stevens, Ronald J. Stouffer, and Karl E. Taylor. Overview of the Coupled Model Intercomparison Project Phase 6 (CMIP6) experimental design and organization. *Geoscientific Model Development*, 9(5):1937–1958, 2016. doi: 10.5194/gmd-9-1937-2016.
- [19] Zachary M. Labe and Elizabeth A. Barnes. Detecting climate signals using explainable AI with single-forcing large ensembles. *Journal of Advances in Modeling Earth Systems*, 2021. ISSN 1942-2466. doi: 10.1029/2021ms002464.
- [20] Benjamin A. Toms, Elizabeth A. Barnes, and Imme Ebert-Uphoff. Physically Interpretable Neural Networks for the Geosciences: Applications to Earth System Variability. *Journal of Advances in Modeling Earth Systems*, 12(9), 2020. ISSN 1942-2466. doi: 10.1029/2019ms002002.
- [21] Stephan Rasp, Peter D. Dueben, Sebastian Scher, Jonathan A. Weyn, Soukayna Mouatadid, and Nils Thuerey. WeatherBench: A Benchmark Data Set for Data-Driven Weather Forecasting. *Journal of Advances in Modeling Earth Systems*, 12(11), 2020. ISSN 1942-2466. doi: 10.1029/2020ms002203.

- [22] Stephan Rasp, Stephan Hoyer, Alexander Merose, Ian Langmore, Peter Battaglia, Tyler Russel, Alvaro Sanchez-Gonzalez, Vivian Yang, Rob Carver, Shreya Agrawal, Matthew Chantry, Zied Ben Bouallegue, Peter Dueben, Carla Bromberg, Jared Sisk, Luke Barrington, Aaron Bell, and Fei Sha. WeatherBench 2: A benchmark for the next generation of data-driven global weather models. *arXiv*, 2023. doi: 10.48550/arxiv.2308.15560.
- [23] Juan Nathaniel, Yongquan Qu, Tung Nguyen, Sungduk Yu, Julius Busecke, Aditya Grover, and Pierre Gentine. ChaosBench: A Multi-Channel, Physics-Based Benchmark for Subseasonal-to-Seasonal Climate Prediction. *arXiv*, 2024. doi: 10.48550/arxiv.2402.00712.
- [24] Jaideep Pathak, Shashank Subramanian, Peter Harrington, Sanjeev Raja, Ashesh Chattopadhyay, Morteza Mardani, Thorsten Kurth, David Hall, Zongyi Li, Kamyar Azizzadenesheli, Pedram Hassanzadeh, Karthik Kashinath, and Animashree Anandkumar. FourCastNet: A Global Data-driven High-resolution Weather Model using Adaptive Fourier Neural Operators. *arXiv*, 2022. doi: 10.48550/arxiv.2202.11214.
- [25] Remi Lam, Alvaro Sanchez-Gonzalez, Matthew Willson, Peter Wirsberger, Meire Fortunato, Ferran Alet, Suman Ravuri, Timo Ewalds, Zach Eaton-Rosen, Weihua Hu, Alexander Merose, Stephan Hoyer, George Holland, Oriol Vinyals, Jacklynn Stott, Alexander Pritzel, Shakir Mohamed, and Peter Battaglia. Learning skillful medium-range global weather forecasting. *Science*, 382(6677):1416–1421, 2023. ISSN 0036-8075. doi: 10.1126/science.adi2336.
- [26] Kaifeng Bi, Lingxi Xie, Hengheng Zhang, Xin Chen, Xiaotao Gu, and Qi Tian. Accurate medium-range global weather forecasting with 3D neural networks. *Nature*, 619(7970):533–538, 2023. ISSN 0028-0836. doi: 10.1038/s41586-023-06185-3.
- [27] Tung Nguyen, Rohan Shah, Hritik Bansal, Troy Arcomano, Sandeep Madireddy, Romit Maulik, Veerabhadra Kotamarthi, Ian Foster, and Aditya Grover. Scaling transformer neural networks for skillful and reliable medium-range weather forecasting. *arXiv*, 2023. doi: 10.48550/arxiv.2312.03876.
- [28] Sungduk Yu, Walter M Hannah, Liran Peng, Mohamed Aziz Bhouiri, Ritwik Gupta, Jerry Lin, Björn Lütjens, Justus C Will, Tom Beucler, Bryce E Harrop, Benjamin R Hillman, Andrea M Jenney, Savannah L Ferretti, Nana Liu, Anima Anandkumar, Noah D Brenowitz, Veronika Eyring, Pierre Gentine, Stephan Mandt, Jaideep Pathak, Carl Vondrick, Rose Yu, Laure Zanna, Ryan P Abernathy, Fiaz Ahmed, David C Bader, Pierre Baldi, Elizabeth A Barnes, Gunnar Behrens, Christopher S Bretherton, Julius J M Busecke, Peter M Caldwell, Wayne Chuang, Yilun Han, Yu Huang, Fernando Iglesias-Suarez, Sanket Jantre, Karthik Kashinath, Marat Khairoutdinov, Thorsten Kurth, Nicholas J Lutsko, Po-Lun Ma, Griffin Mooers, J David Neelin, David A Randall, Sara Shamekh, Akshay Subramanian, Mark A Taylor, Nathan M Urban, Janni Yuval, Guang J Zhang, Tian Zheng, and Michael S Pritchard. ClimSim: An open large-scale dataset for training high-resolution physics emulators in hybrid multi-scale climate simulators. *arXiv*, 2023. doi: 10.48550/arxiv.2306.08754.
- [29] D. Watson-Parris, Y. Rao, D. Olivié, Ø. Seland, P. Nowack, G. Camps-Valls, P. Stier, S. Bouabid, M. Dewey, E. Fons, J. Gonzalez, P. Harder, K. Jeggle, J. Lenhardt, P. Manshausen, M. Novitasari, L. Ricard, and C. Roesch. ClimateBench v1.0: A Benchmark for Data-Driven Climate Projections. *Journal of Advances in Modeling Earth Systems*, 14(10), 2022. ISSN 1942-2466. doi: 10.1029/2021ms002954.
- [30] Julia Kaltenborn, Charlotte E Lange, Venkatesh Ramesh, Philippe Brouillard, Yaniv Gurwicz, Chandni Nagda, Jakob Runge, Peer Nowack, and David Rolnick. ClimateSet: A Large-Scale Climate Model Dataset for Machine Learning. *arXiv*, 2023. doi: 10.48550/arxiv.2311.03721.
- [31] Tung Nguyen, Jason Jewik, Hritik Bansal, Prakhar Sharma, and Aditya Grover. ClimateLearn: Benchmarking Machine Learning for Weather and Climate Modeling. *arXiv*, 2023. doi: 10.48550/arxiv.2307.01909.
- [32] Mark D Zelinka, Timothy A Myers, Daniel T McCoy, Stephen Po-Chedley, Peter M Caldwell, Paulo Ceppi, Stephen A Klein, and Karl E Taylor. Causes of higher climate sensitivity in cmip6 models. *Geophysical Research Letters*, 47(1):e2019GL085782, 2020.

- [33] Gerald A Meehl, Catherine A Senior, Veronika Eyring, Gregory Flato, Jean-Francois Lamarque, Ronald J Stouffer, Karl E Taylor, and Manuel Schlund. Context for interpreting equilibrium climate sensitivity and transient climate response from the cmip6 earth system models. *Science Advances*, 6(26):eaba1981, 2020.
- [34] Alec Radford, Jong Wook Kim, Chris Hallacy, Aditya Ramesh, Gabriel Goh, Sandhini Agarwal, Girish Sastry, Amanda Askell, Pamela Mishkin, Jack Clark, Gretchen Krueger, and Ilya Sutskever. Learning transferable visual models from natural language supervision, 2021.
- [35] Kaiming He, Xinlei Chen, Saining Xie, Yanghao Li, Piotr Dollár, and Ross Girshick. Masked autoencoders are scalable vision learners, 2021.
- [36] Maxime Oquab, Timothée Darcet, Théo Moutakanni, Huy Vo, Marc Szafraniec, Vasil Khalidov, Pierre Fernandez, Daniel Haziza, Francisco Massa, Alaaeldin El-Nouby, Mahmoud Assran, Nicolas Ballas, Wojciech Galuba, Russell Howes, Po-Yao Huang, Shang-Wen Li, Ishan Misra, Michael Rabbat, Vasu Sharma, Gabriel Synnaeve, Hu Xu, Hervé Jegou, Julien Mairal, Patrick Labatut, Armand Joulin, and Piotr Bojanowski. Dinov2: Learning robust visual features without supervision, 2024.
- [37] Muhammad Awais, Muzammal Naseer, Salman Khan, Rao Muhammad Anwer, Hisham Cholakkal, Mubarak Shah, Ming-Hsuan Yang, and Fahad Shahbaz Khan. Foundational models defining a new era in vision: A survey and outlook. *arXiv preprint arXiv:2307.13721*, 2023.
- [38] Ramprasaath R Selvaraju, Michael Cogswell, Abhishek Das, Ramakrishna Vedantam, Devi Parikh, and Dhruv Batra. Grad-cam: Visual explanations from deep networks via gradient-based localization. In *Proceedings of the IEEE international conference on computer vision*, pages 618–626, 2017.

---

**SUPPLEMENTARY INFORMATION**  
for  
**ClimDetect: A Benchmark Dataset for Climate  
Change Detection and Attribution**

---

Sungduk Yu<sup>1\*</sup>, Brian L. White<sup>2</sup>, Anahita Bhiwandiwalla<sup>1</sup>, Musashi Hinck<sup>1</sup>,  
Matthew Lyle Olson<sup>1</sup>, Tung Nguyen<sup>3</sup>, Vasudev Lal<sup>1</sup>

<sup>1</sup>Intel Labs, <sup>2</sup>UNC Chapel Hill, <sup>3</sup>UCLA

## Contents

<b>1</b>	<b>Information for NeurIPS 2024 reviewers</b>	<b>1</b>
<b>2</b>	<b>Model Uncertainty and Resampling Analysis</b>	<b>2</b>
<b>3</b>	<b>Tables</b>	<b>4</b>
3.1	Metrics: $R^2$ . . . . .	4
3.2	CMIP6 Model Information . . . . .	4
<b>4</b>	<b>Figures</b>	<b>6</b>
4.1	Metrics . . . . .	6
4.2	Scatter plots . . . . .	7
4.3	GradCAM Results . . . . .	10
<b>5</b>	<b>Datasheet</b>	<b>14</b>

## 1 Information for NeurIPS 2024 reviewers

- Dataset URL: <https://huggingface.co/datasets/ClimDetect/ClimDetect>
- Croissant metadata URL: <https://huggingface.co/api/datasets/ClimDetect/ClimDetect/croissant>
- The authors accept full responsibility for any violation of rights and confirm adherence to the terms of the CC-BY-4.0 license.

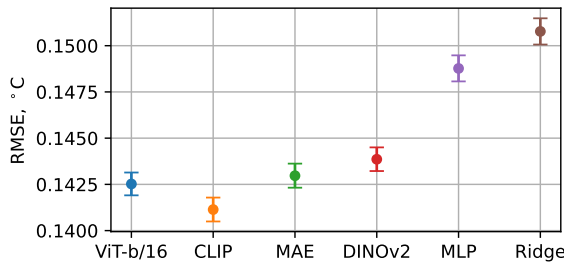
---

\*sungduk.yu@intel.com

- The authors utilize Hugging Face to host the dataset for easy access and commit to providing necessary maintenance. The dataset is locally archived for long-term preservation. In the event of any disruption to the current hosting platform, we will ensure the data is promptly re-uploaded to another suitable platform for open access.

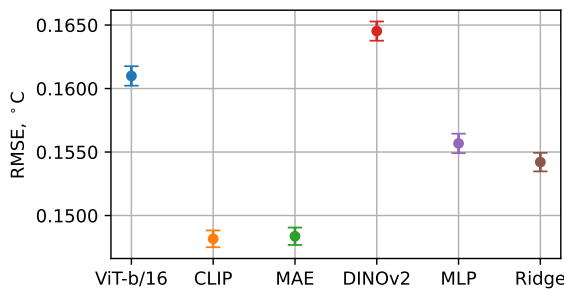
## 2 Model Uncertainty and Resampling Analysis

We employ a bootstrap to estimate the uncertainty associated with our findings in the baseline model analysis. Treating the observations in the test set as randomly drawn from an underlying distribution of climate simulations, we bootstrap our test split 100,000 times to yield a distribution of RMSE values. Based on this distribution, we calculate the median and 95% confidence interval (using the 2.5th and 97.5th percentiles).<sup>2</sup> These results are documented in InfoPanels 1-6, showing the robustness of our baseline model evaluation presented in Table 2 of the main text.



Model	Value
ViT-b/16	0.1425 [0.1419, 0.1431]
CLIP	0.1411 [0.1405, 0.1418]
MAE	0.1430 [0.1423, 0.1436]
DINOv2	0.1439 [0.1432, 0.1445]
MLP	0.1488 [0.1481, 0.1495]
Ridge	0.1508 [0.1501, 0.1515]

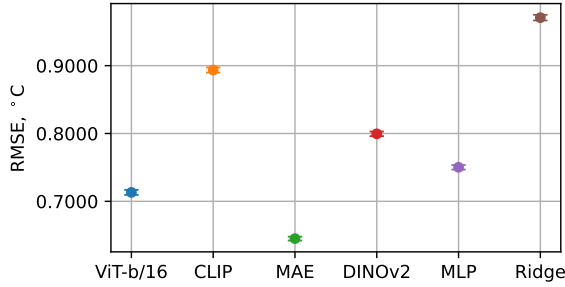
InfoPanel 1: RMSE with 95% confidence intervals for **tas-huss-pr** experiment, estimated via bootstrapping with 100,000 repetitions. On the left, dots represent the medians, and error bars indicate the confidence intervals, spanning from the 2.5th to the 97.5th percentiles. On the right, the median RMSE is depicted alongside its 95% confidence interval in square brackets.



Model	RMSE
ViT-b/16	0.1610 [0.1602, 0.1618]
CLIP	0.1482 [0.1475, 0.1488]
MAE	0.1484 [0.1477, 0.1491]
DINOv2	0.1645 [0.1638, 0.1653]
MLP	0.1557 [0.1549, 0.1564]
Ridge	0.1542 [0.1535, 0.1549]

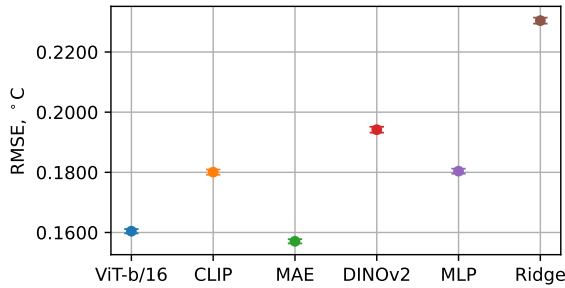
InfoPanel 2: Similar to InfoPanel 1, but for the **tas\_only** experiment

<sup>2</sup>The alternative approach of re-training the model using different starting seeds treats the model as random, and measures uncertainty due to different initializations. Our statistic treats the model as fixed but data as random.



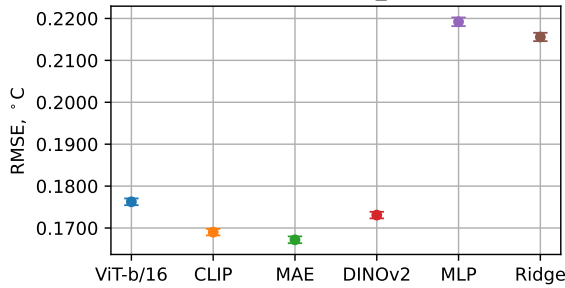
Model	RMSE
ViT-b/16	0.7132 [0.7095, 0.7169]
CLIP	0.8935 [0.8898, 0.8973]
MAE	0.6451 [0.6422, 0.6479]
DINOv2	0.7995 [0.7961, 0.8029]
MLP	0.7502 [0.7469, 0.7535]
Ridge	0.9707 [0.9666, 0.9749]

InfoPanel 3: Similar to InfoPanel 1, but for the **pr\_only** experiment



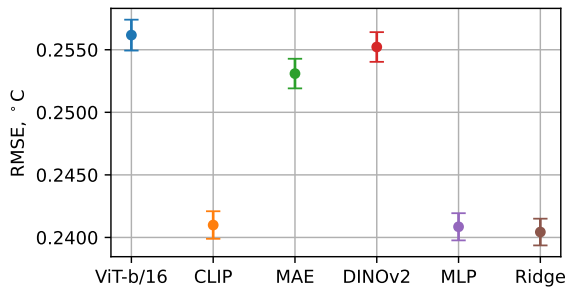
Model	RMSE
ViT-b/16	0.1604 [0.1597, 0.1611]
CLIP	0.1801 [0.1792, 0.1809]
MAE	0.1571 [0.1564, 0.1578]
DINOv2	0.1942 [0.1932, 0.1951]
MLP	0.1804 [0.1796, 0.1812]
Ridge	0.2304 [0.2294, 0.2314]

InfoPanel 4: Similar to InfoPanel 1, but for the **huss\_only** experiment



Model	RMSE
ViT-b/16	0.1763 [0.1754, 0.1771]
CLIP	0.1690 [0.1682, 0.1698]
MAE	0.1672 [0.1664, 0.1680]
DINOv2	0.1731 [0.1723, 0.1739]
MLP	0.2192 [0.2182, 0.2202]
Ridge	0.2156 [0.2146, 0.2166]

InfoPanel 5: Similar to InfoPanel 1, but for the **tas-huss-pr\_mr** experiment



Model	RMSE
ViT-b/16	0.2562 [0.2549, 0.2574]
CLIP	0.2410 [0.2399, 0.2421]
MAE	0.2531 [0.2519, 0.2543]
DINOv2	0.2552 [0.2540, 0.2564]
MLP	0.2409 [0.2398, 0.2419]
Ridge	0.2404 [0.2394, 0.2415]

InfoPanel 6: Similar to InfoPanel 1, but for the **tas\_mr** experiment

### 3 Tables

#### 3.1 Metrics: $R^2$

Model	$R^2$					
	tas-huss-pr	tas_only	pr_only	huss_only	tas-huss-pr_mr	tas_mr
ViT-b/16	0.9847	0.9805	0.6173	0.9806	0.9766	0.9506
CLIP	<b>0.9850</b>	<b>0.9835</b>	0.3992	0.9756	0.9785	0.9563
MAE	0.9846	0.9834	<b>0.6869</b>	<b>0.9814</b>	<b>0.9790</b>	0.9518
DINOv2	0.9844	0.9796	0.5190	0.9716	0.9775	0.9510
MLP	0.9833	0.9818	0.5765	0.9755	0.9638	0.9563
Ridge	0.9829	0.9821	0.2909	0.9600	0.9650	<b>0.9565</b>

Table 1: Similar to Table 2 of the main text, but for the coefficient of determination

#### 3.2 CMIP6 Model Information

model	Test Set		
	scenario	grid	ensemble members
ACCESS-CM2	historical	gn	rlilplfl
	ssp245	gn	rlilplfl
	ssp370	gn	rlilplfl
CMCC-CM2-SR5	historical	gn	rlilplfl
	ssp245	gn	rlilplfl
	ssp370	gn	rlilplfl
CMCC-ESM2	historical	gn	rlilplfl
	ssp245	gn	rlilplfl
	ssp370	gn	rlilplfl
FGOALS-g3	historical	gn	rlilplfl
	ssp245	gn	rlilplfl
GFDL-CM4	historical	gr1	rlilplfl
	ssp245	gr1, gr2	rlilplfl
GFDL-ESM4	historical	gr1	rlilplfl
	ssp245	gr1	rlilplfl
	ssp370	gr1	rlilplfl
IITM-ESM	historical	gn	rlilplfl
	ssp370	gn	rlilplfl

Table 2: Details of CMIP6 simulations incorporated in the test set

				Training Set
model	scenario	grid	ensemble members	
CESM2	historical	gn	r1i1p1f1, r4i1p1f1, r1i1p1f1	
	ssp245	gn	r4i1p1f1, r10i1p1f1, r1i1p1f1	
	ssp370	gn	r4i1p1f1, r10i1p1f1, r1i1p1f1	
CNRM-CM6-1	historical	gr	r1i1p1f2	
	ssp245	gr	r1i1p1f2	
	ssp370	gr	r1i1p1f2	
CNRM-ESM2-1	historical	gr	r1i1p1f2	
	ssp245	gr	r1i1p1f2	
	ssp370	gr	r1i1p1f2	
CanESM5	historical	gn	r1i1p1f1, r2i1p1f1, r3i1p1f1, r1i1p2f1, r2i1p2f1, r3i1p2f1	
	ssp245	gn	r1i1p1f1, r2i1p1f1, r3i1p1f1, r1i1p2f1, r2i1p2f1, r3i1p2f1	
	ssp370	gn	r1i1p1f1, r2i1p1f1, r3i1p1f1, r1i1p2f1, r2i1p2f1, r3i1p2f1	
EC-Earth3	historical	gr	r1i1p1f1, r4i1p1f1, r7i1p1f1	
	ssp245	gr	r1i1p1f1, r4i1p1f1, r7i1p1f1	
	ssp370	gr	r1i1p1f1, r4i1p1f1, r150i1p1f1	
EC-Earth3-CC	historical	gr	r1i1p1f1	
	ssp245	gr	r1i1p1f1	
EC-Earth3-Veg	historical	gr	r1i1p1f1, r4i1p1f1	
	ssp245	gr	r1i1p1f1, r4i1p1f1, r6i1p1f1	
	ssp370	gr	r1i1p1f1, r4i1p1f1	
EC-Earth3-Veg-LR	historical	gr	r1i1p1f1, r2i1p1f1, r3i1p1f1	
	ssp245	gr	r1i1p1f1, r2i1p1f1, r3i1p1f1	
	ssp370	gr	r1i1p1f1, r2i1p1f1, r3i1p1f1	
HadGEM3-GC31-LL	historical	gn	r1i1p1f3	
	ssp245	gn	r1i1p1f3	
INM-CM4-8	historical	gr1	r1i1p1f1	
	ssp245	gr1	r1i1p1f1	
	ssp370	gr1	r1i1p1f1	
INM-CM5-0	historical	gr1	r1i1p1f1, r2i1p1f1, r3i1p1f1	
	ssp245	gr1	r1i1p1f1	
	ssp370	gr1	r1i1p1f1, r2i1p1f1, r3i1p1f1, r4i1p1f1, r5i1p1f1	
MIROC-ES2L	historical	gn	r1i1p1f2	
	ssp245	gn	r1i1p1f2	
MPI-ESM1-2-HR	historical	gn	r1i1p1f1, r2i1p1f1, r3i1p1f1	
	ssp245	gn	r1i1p1f1, r2i1p1f1	
	ssp370	gn	r1i1p1f1, r2i1p1f1, r3i1p1f1, r4i1p1f1	
MPI-ESM1-2-LR	historical	gn	r1i1p1f1, r2i1p1f1, r3i1p1f1	
	ssp245	gn	r1i1p1f1, r2i1p1f1	
	ssp370	gn	r1i1p1f1, r2i1p1f1, r3i1p1f1, r4i1p1f1	
NorESM2-LM	historical	gn	r1i1p1f1, r2i1p1f1	
	ssp245	gn	r1i1p1f1, r2i1p1f1, r3i1p1f1	
	ssp370	gn	r1i1p1f1	
UKESM1-0-LL	historical	gn	r1i1p1f2, r2i1p1f2, r3i1p1f2	
	ssp245	gn	r1i1p1f2, r2i1p1f2, r3i1p1f2	
	ssp370	gn	r1i1p1f2, r2i1p1f2, r3i1p1f2	

Table 3: Details of CMIP6 simulations incorporated in the training set

Validation Set			
model	scenario	grid	ensemble members
CESM2-WACCM	historical	gn	r1i1p1f1
	ssp245	gn	r1i1p1f1
	ssp370	gn	r1i1p1f1
KACE-1-0-G	historical	gr	r1i1p1f1
	ssp245	gr	r1i1p1f1
	ssp370	gr	r1i1p1f1
MRI-ESM2-0	historical	gn	r1i1p1f1
	ssp245	gn	r1i1p1f1
	ssp370	gn	r1i1p1f1
NorESM2-MM	historical	gn	r1i1p1f1
	ssp245	gn	r1i1p1f1
	ssp370	gn	r1i1p1f1
TaiESM1	historical	gn	r1i1p1f1
	ssp245	gn	r1i1p1f1

Table 4: Details of CMIP6 simulations incorporated in the validation set

## 4 Figures

### 4.1 Metrics

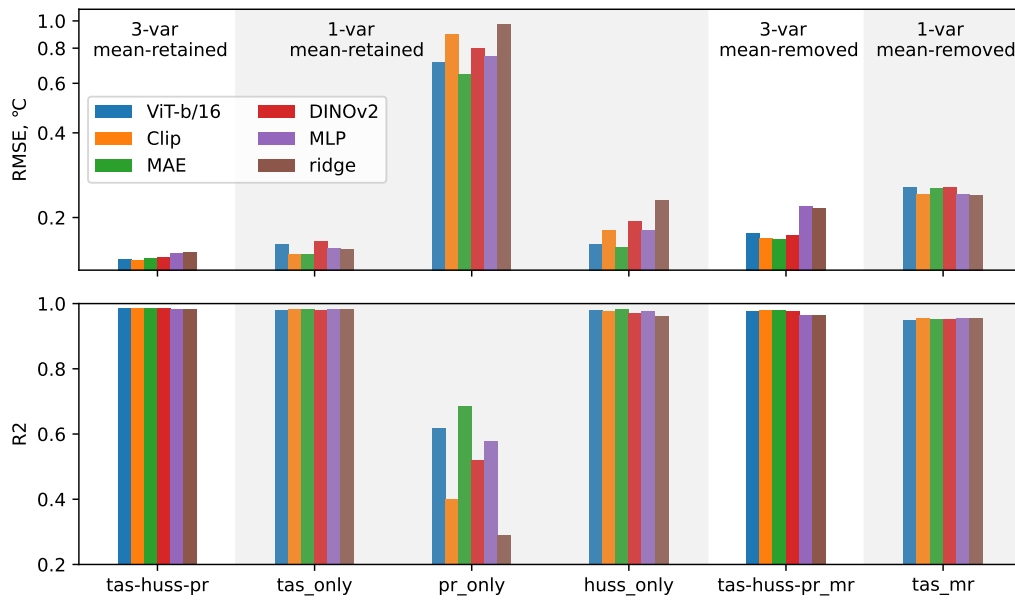


Figure 1: (top) RMSE; (bottom) Coefficient of determination, R<sup>2</sup>.

## 4.2 Scatter plots

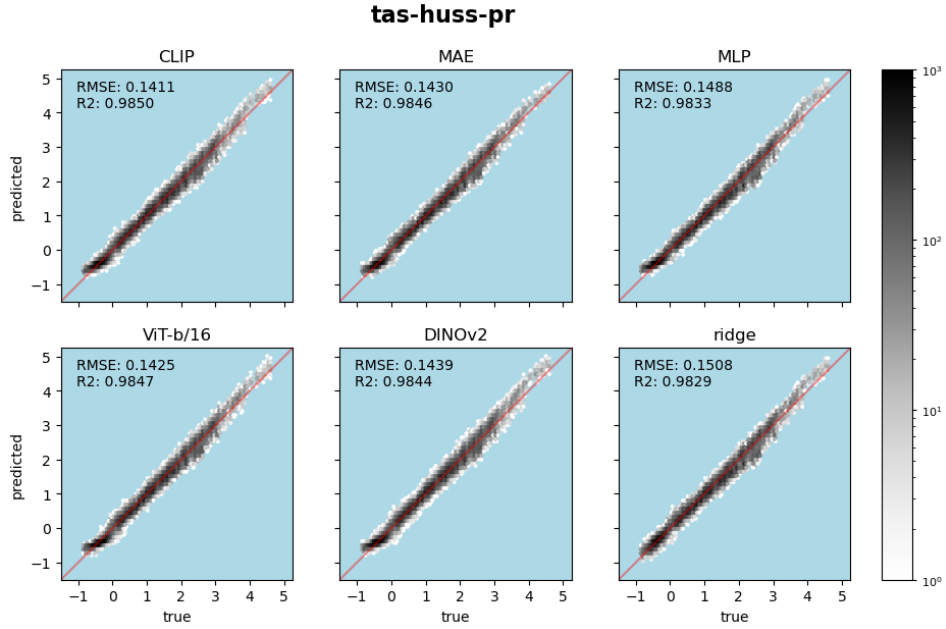


Figure 2: Comparison of model predictions for **tas-huss-pr** experiment using hexagonal binning (hexbin) plots. Each panel represents a hexbin plot of the predicted versus true values from a different model (CLIP, MAE, ViT-b/16, DINOv2, MLP, and Ridge). The red line indicates perfect prediction alignment. Root mean square Error (RMSE) and coefficient of determination ( $R^2$ ) values are displayed in the upper right corner of each subpanel.

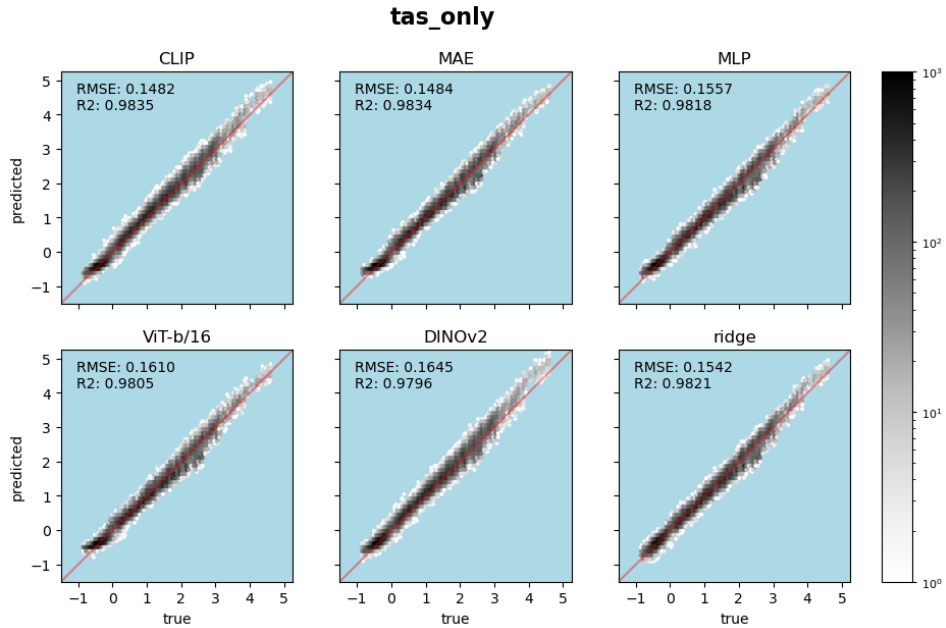


Figure 3: Similar to Figure 2, but for **tas\_only** experiment.

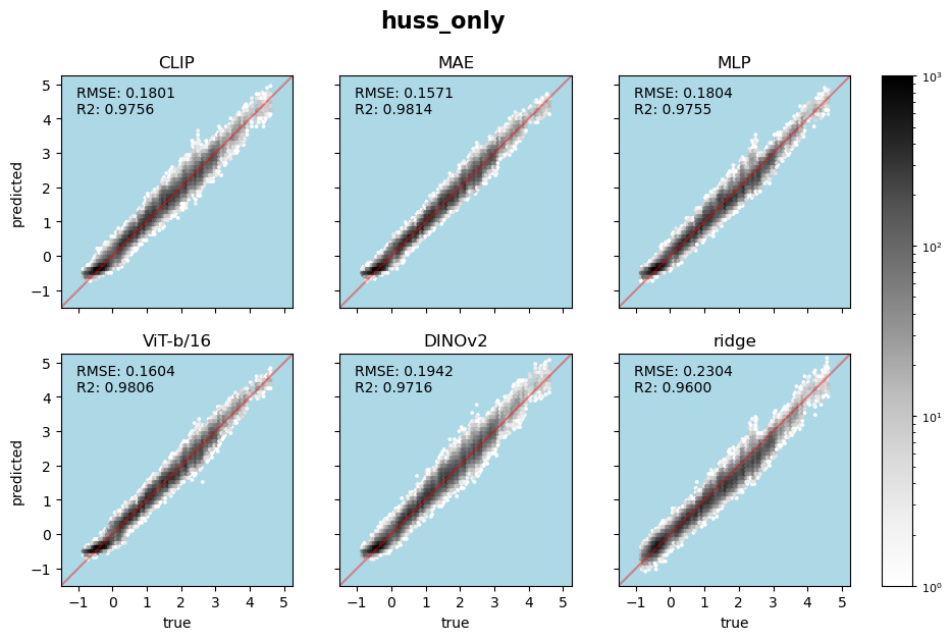


Figure 4: Similar to Figure 2, but for **huss\_only** experiment.

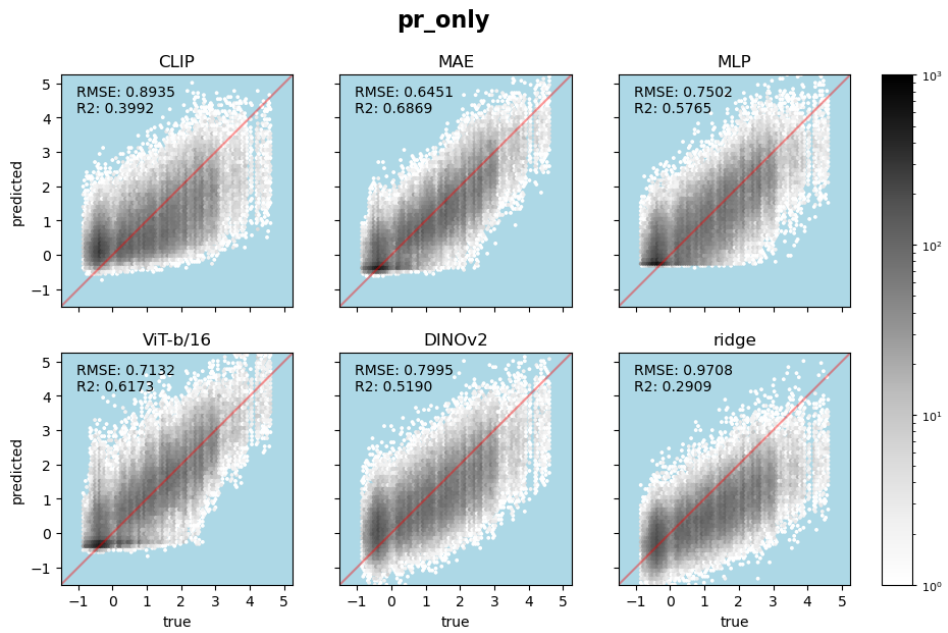


Figure 5: Similar to Figure 2, but for **pr\_only** experiment.

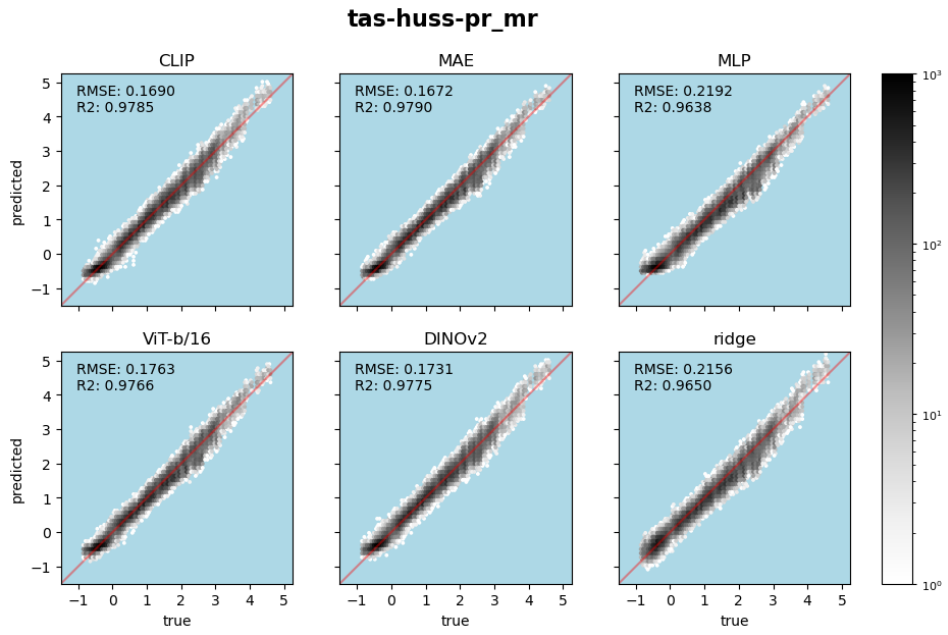


Figure 6: Similar to Figure 2, but for **tas-huss-pr\_mr** experiment.

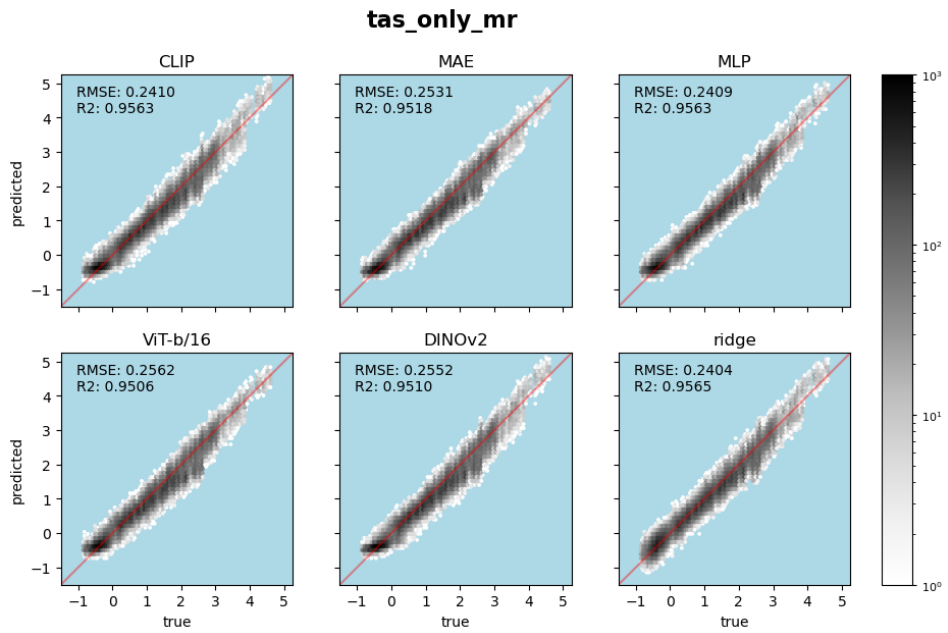


Figure 7: Similar to Figure 2, but for **tas\_mr** experiment.

### 4.3 GradCAM Results

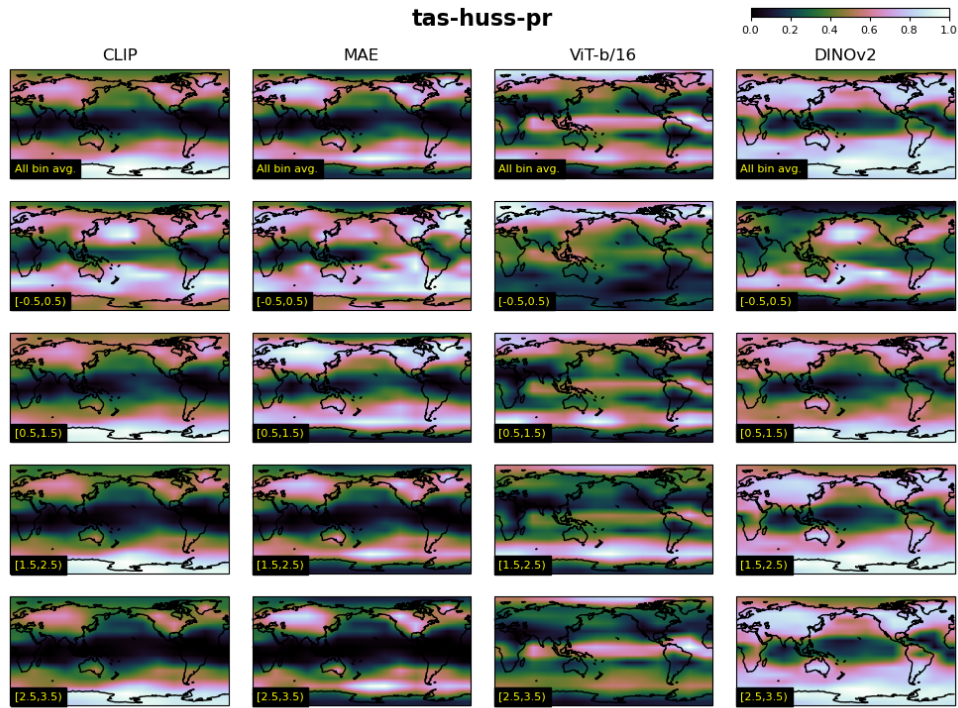


Figure 8: Grad-CAM visualizations across multiple models and AGMT bins for **tas-huss-pr** experiment. Each column represents a different ViT model (CLIP, MAE, ViT-b/16, and DINOv2), while each row corresponds to a specific range of AGMT values, indicated in the bottom left corner of each subpanel. Grad-CAM was calculated for test set samples falling within each AGMT bin, and the results were then averaged before making visualizations.

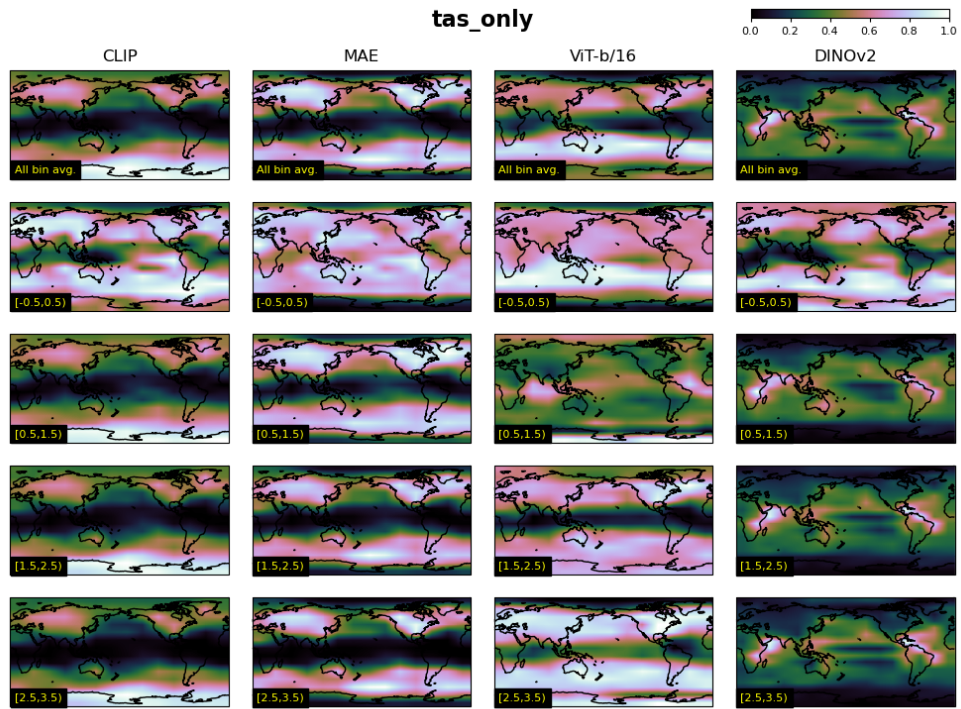


Figure 9: Similar to Figure 8, but for **tas\_only** experiment.

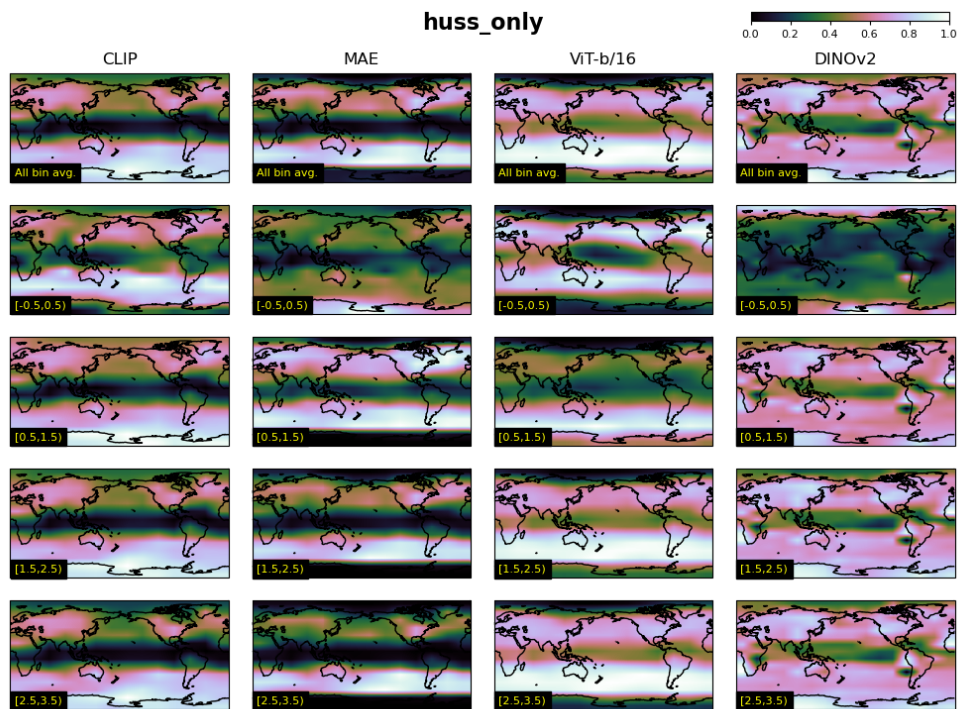


Figure 10: Similar to Figure 8, but for **huss\_only** experiment.

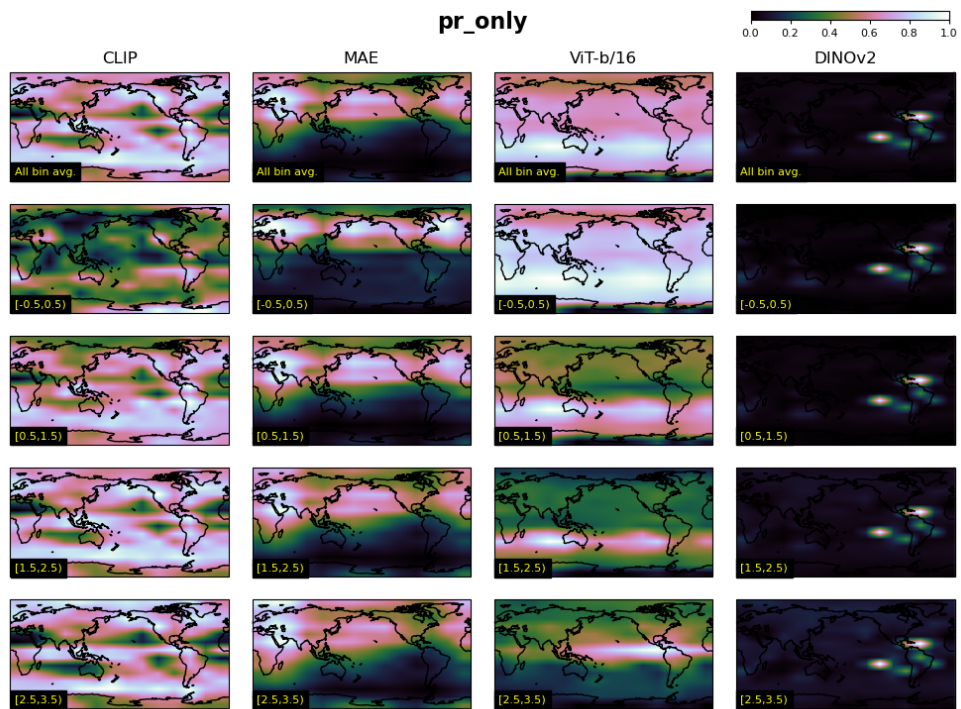


Figure 11: Similar to Figure 8, but for **pr\_only** experiment.

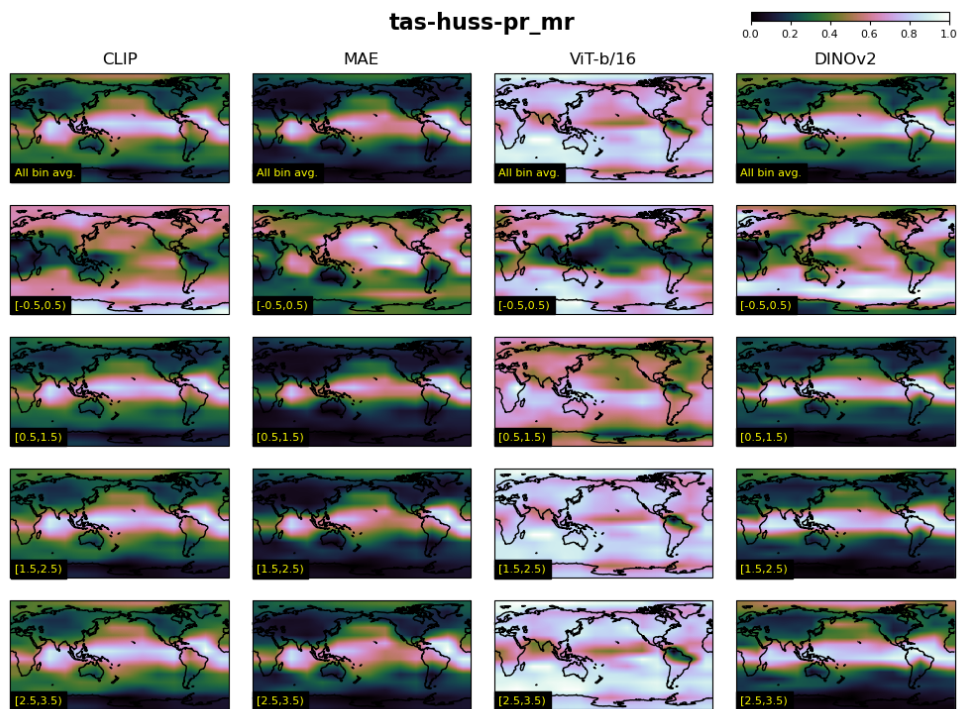


Figure 12: Similar to Figure 8, but for **tas-huss-pr\_mr** experiment.

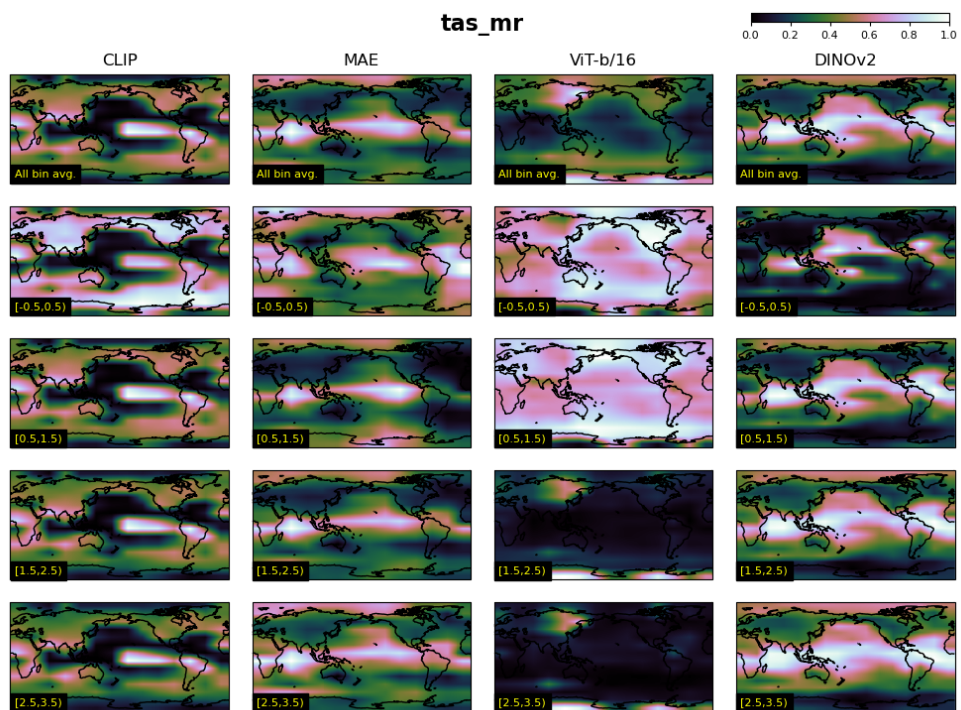


Figure 13: Similar to Figure 8, but for **tas\_mr** experiment.

## 5 Datasheet

### Motivation

- **For what purpose was the dataset created?** *ClimDetect* dataset was created to standardize the detection and attribution of climate change signals by integrating various input and target variables used in past research, addressing the gap in consistent comparisons across studies, and exploring the application of vision transformers to climate data for improved model evaluations.
- **Who created the dataset (e.g., which team, research group) and on behalf of which entity (e.g., company, institution, organization)?** A consortium of climate scientists and ML/AI researchers from Intel Labs (a research and development organization within Intel Corporation) and academic institutions (UNC Chapel Hill and UCLA) created the dataset.
- **Who funded the creation of the dataset?** The creation of this dataset was funded by Intel Corporation.

### Composition

- **What do the instances that comprise the dataset represent (e.g., documents, photos, people, countries)?** The instances in the dataset represent daily global climate snapshots (for near-surface temperature, near-surface specific humidity, and total precipitation rate) their associated annual global mean temperature and year.
- **How many instances are there in total?** There are 816,213 instances in the dataset.
- **Does the dataset contain all possible instances or is it a sample (not necessarily random) of instances from a larger set?** The dataset contain all possible instances based on the selection process described in Section 3.1.
- **What data does each instance consist of?** Each instance consists of "raw" climate simulation outputs in the form of an image-like format ([latitude, longitude] instead of [height, width]).
- **Is there a label or target associated with each instance? If so, please provide a description.** Each instance has associated targets, specifically designed for climate change detection, such as the Annual Global Mean Temperature (AGMT) and year
- **Is any information missing from individual instances?** There is no information missing from the instances in a manner that impacts the dataset's utility for its intended use.
- **Are relationships between individual instances made explicit (e.g., users' movie ratings, social network links)?** Relationships between instances (e.g., temporal sequence of climate snapshots) are not made explicit within the dataset as each snapshot is treated independently for the purpose of model training and validation.
- **Are there recommended data splits (e.g., training, development/validation, testing)?** 77% of the samples (627,581 samples) are allocated to the training dataset, 10% (80,227 samples) to the validation dataset, and the remaining 13% (108,405 samples) to the testing dataset.
- **Are there any errors, sources of noise, or redundancies in the dataset?** There are no known errors or redundancies in the dataset. Any noise present is inherent to the climatic simulation data due to the factors such as model physics, numerical schemes, initial and boundary conditions.
- **Is the dataset self-contained, or does it link to or otherwise rely on external resources (e.g., websites, tweets, other datasets)?** The dataset is self-contained.

- **Does the dataset contain data that might be considered confidential (e.g., data that is protected by legal privilege or by doctor– patient confidentiality, data that includes the content of individuals’ non-public communications)?** *The dataset does not contain confidential information. It is composed of climate data, which does not include personal, sensitive, or offensive content.*

### Collection Process

- **Where was the data collected at?** *The data was not collected from a physical location but was derived from the CMIP6 climate models, which are internationally contributed by various climate research centers.*
- **If the dataset is a sample from a larger set, what was the sampling strategy?** *The dataset is not a random sample but a curated selection from CMIP6 intended to standardize climate change detection efforts. See Section 3.1 for the detailed curation criteria.*
- **Are there any guarantees that the acquisition of the data did not violate any law or anyone’s rights?** *This data is sourced from publicly available climate model outputs that are freely accessible for scientific research. To the best of our knowledge this data does not violate any law or anyone’s rights.*
- **Are there any guarantees that prove the data is reliable?** *The reliability of the data in ClimDetect is ensured by the rigorous scientific processes inherent in the CMIP6 protocol, which is recognized by the international climate modeling community.*
- **Did the collection process involve the participation of individual people?** *No.*
- **Has an analysis of the potential impact of the dataset and its use on data subjects been conducted?** *Given that the dataset comprises climate model data and not personal data, a data protection impact analysis is not applicable.*
- **Were any ethical review processes conducted?** *No specific ethical review was necessary for the dataset as it involves no human subjects or ethically sensitive content.*
- **Does the data come from a single source or is it the result of a combination of data coming from different sources? In any case, please provide references.** *The source data comes from a combination of different sources, e.g., climate modeling centers from different countries, but they all adhere to the same CMIP6 simulation protocol.*
- **If the same content was to be collected from a different source, would it be similar?** *The content would likely be similar due to the standardized nature of global climate modeling practices.*

### Preprocessing/Cleaning/Labelling

- **Please specify any information regarding the preprocessing that you may know (e.g. the person who created the dataset has somehow explained it) or be able to find (e.g. there exists and informational site).** *The preprocessing details of the dataset are documented in Section 3.2*
- **Was the “raw” data saved in addition to the preprocessed/cleaned/labeled data (e.g., to support unanticipated future uses)?** *The raw data is not stored locally but is archived in multiple public repositories, including LLNL-ESGF (<https://esgf.llnl.gov>), AWS-ASDI (<https://registry.opendata.aws/cmip6>), and Google Cloud (<https://console.cloud.google.com/storage/browser/cmip6>).*
- **Is the software that was used to preprocess/clean/label the data available?** *Python (<https://www.python.org>), CDO (<https://code.mpimet.mpg.de/projects/>)*

*cdo/*), NCO (<https://nco.sourceforge.net>), and GNU Parallel (<https://www.gnu.org/software/parallel/>) were used to preprocess the dataset.

## Uses

- **Has the dataset been used already? If so, please provide a description.** *The dataset has been utilized in training the baseline models in Section 4.*
- **Is there a repository that links to any or all papers or systems that use this dataset? If so, please provide a link or any other access point.** *Currently, there is no specific repository linking to papers or systems that use this dataset. As the dataset and related research are newly developed, relevant publications and resources will be compiled and shared as they become available through the dataset repository on HuggingFace.*
- **What (other) tasks could the dataset be used for? Please include your own intentions, if any.** *The ClimDetect dataset is primarily tailored for climate science applications but could also be adapted for educational use in data science and environmental studies.*
- **Are there tasks for which the dataset should not be used? If so, please provide a description.** *The ClimDetect dataset is specifically tailored for climate science and lacks relevance for non-climate related fields, offering no actionable insights in such areas.*

## Distribution

- **Please specify the source where you got the dataset from.** *The ClimDetect dataset is compiled from climate model outputs part of the Coupled Model Intercomparison Project Phase 6 (CMIP6), which is coordinated by the World Climate Research Programme (WCRP). See Section 3.1 for details*
- **When was the dataset first released?** *The ClimDetect dataset was released in June 2024.*
- **Are there any restrictions regarding the distribution and/or usage of this data in any particular geographic regions?** *There are no geographic restrictions on the distribution or usage of the dataset.*
- **Is the dataset distributed under a copyright or other intellectual property (IP) license?** *The dataset is distributed under CC-BY-4.0 license.*

## Maintenance

- **Is there any verified manner of contacting the creator of the dataset?** *The dataset creators can be contacted via the official project email listed in the author information of the manuscript.*
- **Specify any limitations there might be to contributing to the dataset. i.e. Can anyone contribute to it? Can someone do it at all?** *Contributions to the ClimDetect dataset are welcome.*
- **Has any erratum been notified?** *As of June 2024, no errata have been reported*
- **Is there any verified information on whether the dataset will be updated in any form in the future?** *There are no scheduled updates for the ClimDetect dataset; however, any identified errors will be corrected, updated, and documented transparently on the dataset's repository website.*
- **Is there any available log about the changes performed previously in the dataset?** *Currently, there is no change log as the ClimDetect dataset has just been released. However, we will document and publish all updates and changes, including error fixes, as necessary.*

- **Could changes to current legislation end the right-of-use of the dataset?** *While the dataset is robustly protected under the CC-BY-4.0 license, significant legal changes could necessitate a review of usage rights.*